

# Imidazolium-based co-poly(ionic liquid) membranes for CO<sub>2</sub>/N<sub>2</sub> separation

Nellepalli Pothanagandhi<sup>a</sup>, Liliana C. Tomé<sup>b,‡</sup>, Kari  
Vijayakrishna<sup>\*a</sup>, Isabel M. Marrucho<sup>\*b,c</sup>

*<sup>a</sup>Department of Chemistry, School of Advanced Sciences, VIT University, Vellore  
632014, Tamil Nadu, India*

*<sup>b</sup>Instituto de Tecnologia Química e Biológica, Universidade Nova de Lisboa, Av.  
República, 2780-157 Oeiras, Portugal.*

*<sup>c</sup>Centro de Química Estrutural, Departamento de Engenharia Química, Instituto  
Superior Técnico, Universidade de Lisboa, Avenida Rovisco Pais, 1049-001 Lisboa,  
Portugal.*

**\*Corresponding Authors:**

Kari Vijayakrishna, Phone: +91 416 224 2334, Fax: +91 416 224 3092 E-mail:  
kari@vit.ac.in, vijayakrishnakari@gmail.com

Isabel M. Marrucho, Phone: +351-218413385, E-mail: [isabel.marrucho@tecnico.ulisboa.pt](mailto:isabel.marrucho@tecnico.ulisboa.pt)

**‡ Present address:** POLYMAT, University of the Basque Country UPV/EHU, Joxe Mari  
Korta Center, Avda. Tolosa 72, 20018 Donostia-San Sebastian, Spain.

## **ABSTRACT**

The development of efficient carbon dioxide capture and separation technologies is at the fore front of the priorities in the climate change policies. Poly(ionic liquid)s (PILs) have been emerging as extremely promising materials for the fabrication of membranes for CO<sub>2</sub> separation. This work is a step forward to evaluate the performance of PIL-based copolymers in the preparation of membranes for CO<sub>2</sub>/N<sub>2</sub> separation. In particular, imidazolium-based homo and copolymers were synthesized by RAFT co-polymerization of different imidazolium salts and characterized by nuclear magnetic resonance (NMR), differential scanning calorimetry (DSC) and thermogravimetric analysis (TGA) analysis. The membrane forming ability of the synthesized PILs, as well as the influence of different side chain groups (ethyl, pentyl, benzyl and naphthyl) at imidazolium ring, were evaluated using the solvent casting technique. In order to improve membrane forming ability and CO<sub>2</sub> separation performance, different amounts of free ionic liquid (IL), [C<sub>2</sub>mim][NTf<sub>2</sub>], were added into the synthesized homo and copolymers, and PIL–IL composite membranes were prepared. The CO<sub>2</sub> and N<sub>2</sub> permeation properties of the obtained free standing PIL–IL membranes were measured at 20 °C and 100 kPa and the results obtained compared through the Robeson plot.

## **KEYWORDS**

Poly(ionic liquid)s; PIL-based copolymers; PIL–IL composite membranes; Gas transport; CO<sub>2</sub>/N<sub>2</sub> separation.

## 1. INTRODUCTION

The development of new materials for carbon dioxide (CO<sub>2</sub>) capture is becoming of vital importance as concerns on the growing concentration of anthropogenic CO<sub>2</sub>, associated to global warming and unpredictable climate changes are being widely expressed. In particular, considerable attention has been paid to ionic liquids (ILs), due to the unique tunability of their properties<sup>1-2</sup> and superior CO<sub>2</sub> affinity in comparison with light gases, such as N<sub>2</sub> and CH<sub>4</sub>.<sup>3-4</sup> Several approaches have been proposed: from mixtures of ILs with other solvents, such as amines<sup>5</sup> and glycols,<sup>6</sup> to functionalization of ILs with diverse chemical groups,<sup>7-12</sup> to other more sophisticated methodologies, as for instance ILs impregnation on different porous supports, such as polymeric membranes,<sup>13-14</sup> zeolites,<sup>15</sup> silica gel,<sup>16</sup> metal-organic frameworks.<sup>17</sup>

In what concerns the use of ILs in membranes, two strategies deserve special attention: the use of an inert porous membrane to support ILs and the incorporation of ILs in a polymeric matrix. Supported ionic liquid membranes (SILMs) have been widely studied for CO<sub>2</sub> separation as they offer a facile preparation methodology.<sup>18</sup> Results using a large number of ILs show that SILMs is a very promising strategy since high CO<sub>2</sub> permeabilities and attractive permselectivities can be obtained. However, SILMs present a major drawback: their low stability under high trans-membrane pressures and high temperatures, due to the weak capillary forces that hold the ILs within the pores. On the other hand, the incorporation of ILs in polymeric membranes, in which the IL is entrapped in the tight spaces between the polymer chains, has proved to be a successful approach, providing membranes with increased mechanical strength compared to SILMs. A large variety of common polymers has been used to prepare polymer-IL composites,<sup>19-21</sup> but the most successful approach lays on the use of poly(ionic liquid)s (PILs),<sup>22-23</sup> since they allow the incorporation of higher amounts of ILs, due to the large degree of strong ionic interactions between the IL and the PIL components.

On top of that, neat PIL membranes possess higher CO<sub>2</sub> sorption capacities than their corresponding IL monomers,<sup>24</sup> and present CO<sub>2</sub>/CH<sub>4</sub> and CO<sub>2</sub>/N<sub>2</sub> on par or greater than those observed for SILMs.<sup>23, 25-27</sup>

The gas permeation properties of PIL membranes are strongly influenced by the structures of the polymer backbone and/or polycation,<sup>28-30</sup> the substituent at the quaternized atom,<sup>22-23, 25, 27, 30-34</sup> and the anion.<sup>23, 35-37</sup> Gas permeation properties through PIL–IL composite membranes based on PILs bearing different cation functionalities, such as imidazolium, pyridinium, pyrrolidinium, ammonium and cholinium, have been investigated. The results showed that although PIL–IL membranes based on pyridinium-based PIL exhibited the highest CO<sub>2</sub> permeability (20.4 Barrer), the greatest CO<sub>2</sub>/CH<sub>4</sub> (43.0) and CO<sub>2</sub>/N<sub>2</sub> (34.7) permselectivities were found for membranes comprising the PIL cholinium.<sup>30</sup> Moreover, PIL–IL membranes containing different anions, such as dicyanamide ([N(CN)<sub>2</sub>]<sup>-</sup>), tricyanomethane ([C(CN)<sub>3</sub>]<sup>-</sup>), tetracyanoborate ([B(CN)<sub>4</sub>]<sup>-</sup>) and bis(trifluoromethylsulfonyl) imide ([NTf<sub>2</sub>]<sup>-</sup>), were studied and it was concluded that the anion also influences both CO<sub>2</sub> permeabilities and CO<sub>2</sub>/N<sub>2</sub> permselectivities [23, 35, 36, 38].<sup>23, 35-36, 38</sup>

Most of the PIL-based membranes developed for CO<sub>2</sub> separation use imidazolium-based PILs as polymer matrices,<sup>39</sup> due to the simplicity of the base ion, ease of modification and wide variety of chemistries available. Noble's group has developed numerous membranes using imidazolium-based PILs, ranging from neat PILs, to gemini and polar-substituted PILs. These solid dense membranes showed CO<sub>2</sub> permeability values from 4 to 30 Barrer and CO<sub>2</sub>/N<sub>2</sub> permselectivities between 30 and 40.<sup>25-27</sup> In order to improve the CO<sub>2</sub> separation performance of PIL imidazolium-based membranes, several strategies have been proposed being the use of composite structures containing both PILs and ILs the most successful one. It has been shown that the incorporation of 20 wt% of a free IL into an imidazolium-based PIL can lead to an enhancement in permeability up to 400 %.<sup>22</sup> In order to increase the amount of

free IL without severely compromising mechanical stability, IL-based cross-linkers can be used. For example, Li *et al.* incorporated up to 60 wt% of free IL into poly(vinylimidazolium) membrane materials,<sup>40</sup> while Carlisle *et al.* made cross-linked poly(vinylimidazolium) membranes with 75 wt% of free IL.<sup>41</sup>

The design of membranes with PIL copolymers is an alternative strategy for CO<sub>2</sub> separation. The structures of PIL copolymers, which have been developed for this purpose, are given in Figure 1.

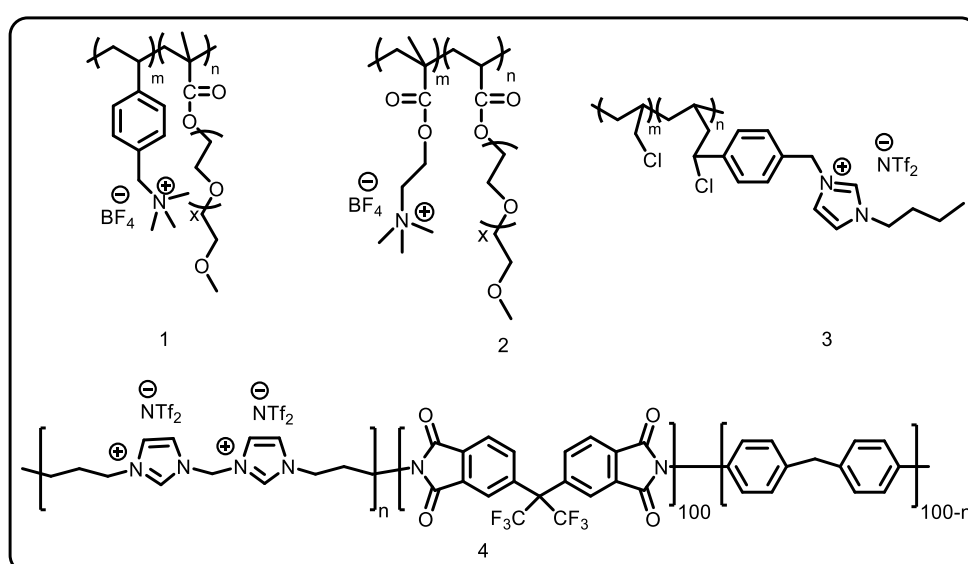


**Figure 1** Different PIL copolymers structures which have been used to develop CO<sub>2</sub> separation membranes.

Radosz and his co-workers developed membranes with PIL copolymers made by grafting of poly(ethylene glycol) onto ammonium-based PILs.<sup>42</sup> The obtained membranes were found to be chemically and mechanically stable and shown CO<sub>2</sub> permeabilities as high as 40 Barrer (at 351 °C) with CO<sub>2</sub>/N<sub>2</sub> permselectivities up to 70.<sup>42</sup> Later, Li *et al.* prepared different random copolyimides using di-amino functional ILs and made free standing membranes by solvent casting technique. The influence of free volume raised by aromatic groups in polyimides on gas sorption and diffusion behavior was investigated. The incorporation of IL moieties into polyimide backbone decreased the availability of free volume in copolyimides

resulting in a significant decrease of the gas permeabilities compared to those of the pure polyimides.<sup>43</sup> Chi *et al.* proposed CO<sub>2</sub> separation membranes with different graft copolymers, consisting of poly(vinyl chloride) in main chains and imidazolium-based PIL in side chains. In sum, increasing the PIL content in copolymer results increased the CO<sub>2</sub> permeabilities. Nevertheless, a slight decrease in CO<sub>2</sub>/N<sub>2</sub> permselectivities was also observed.<sup>44</sup>

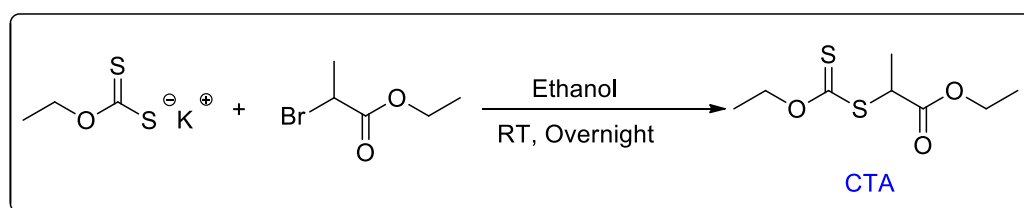
In this work, imidazolium-based homo and co-PILs having different side chain groups (ethyl, pentyl, benzyl and naphthyl) at imidazolium ring were synthesized through RAFT polymerization and characterized. The membrane forming ability of the synthesized PILs and PIL–IL composites, containing different amounts of free [C<sub>2</sub>mim][NTf<sub>2</sub>] IL, was evaluated using the solvent casting technique. The CO<sub>2</sub> and N<sub>2</sub> permeation properties of the obtained free standing PIL–IL membranes were measured using a time lag apparatus and the CO<sub>2</sub>/N<sub>2</sub> separation performance discussed. The goal of this work is to understand the influence of using co-PILs, having different side chain groups (ethyl, pentyl, benzyl and naphthyl) at imidazolium ring, on the stability and gas separation properties of PIL–IL composite membranes.

## 2. EXPERIMENTAL SECTION

**2.1. Materials.** 1-Vinylimidazole (>99%), *n*-bromoethane (98%), *n*-bromopentane (98%), benzyl bromide (98%), styrene, ethyl-2-bromopropionate (99%), 1-(chloromethyl)naphthalene (97%), potassium ethyl xanthogenate (96%) and lithium bis(trifluoromethylsulfonyl)imide salt (LiNTf<sub>2</sub>, 99%) were purchased from Sigma-Aldrich Chemicals (India) and used as received. The 2, 2'-Azo-bis isobutyronitrile (AIBN) was obtained from AVRA Chemicals (India) and recrystallized in methanol before further use. In order that, 3 g of AIBN were taken in 15 mL of methanol and slowly heated until the solid was completely dissolved. Then, the solution was allowed to cool slowly on insulated

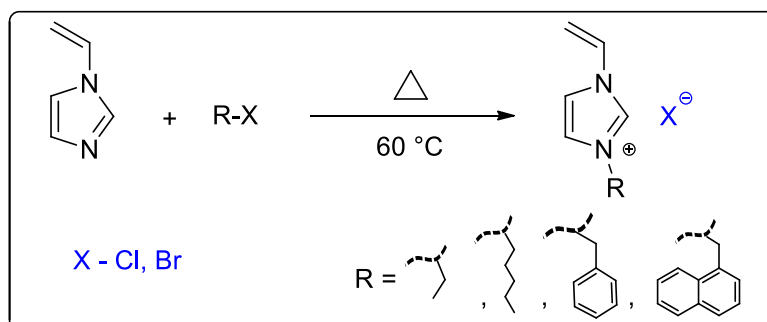
surface. The obtained crystals were filtered and dried under vacuum. All the solvents used were purchased from Rankem Chemicals (India) and distilled prior usage.

**2.2. Synthesis.** The chain transfer agent (CTA), potassium ethyl xanthogenate 1.06 g (6.62 mmol), was first dissolved in ethanol in a round bottom flask, and 1 g of ethyl-2-bromopropionate (5.52 mmol) was added. The mixture was stirred at room temperature (RT) overnight, as depicted in Scheme 1. At the end of the reaction, the 2-ethoxythiocarbonylsulfanyl-propionic acid ethyl ester was obtained (1.13 g, 92% yield).<sup>45</sup>



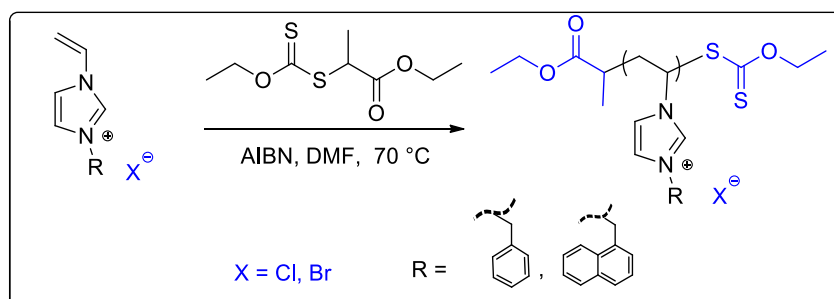
**Scheme 1.** Synthesis of CTA.

The vinylimidazolium-based monomers having different side chains, namely ethyl, pentyl, benzyl and naphthyl were synthesized as described elsewhere.<sup>46</sup> Briefly, the monomer 1-vinyl-3-pentyl imidazolium bromide, (ViPenIm)Br was prepared in quantitative yields by mixing 3 g of 1-vinylimidazole (31.8 mmol) with 7.22 g of *n*-bromopentane (47.81 mmol) in a round bottom flask. The mixture was then allowed to react at 60 °C, in an oil bath for 3 h. The other vinyl monomers were synthesized following the same procedure, as shown in Scheme 2. Nevertheless, in the synthesis of the (ViBenIm)Br monomer, 1-vinylimidazole was initially dissolved in 10 mL of methanol and bromobenzene was added slowly in dropwise portions. This mixture was heated at 60 °C for 3 h and the 1-vinyl-3-benzylimidazolium bromide (ViBenIm)Br was produced in quantitative yield .



**Scheme 2.** Synthesis of vinylimidazolium monomers.

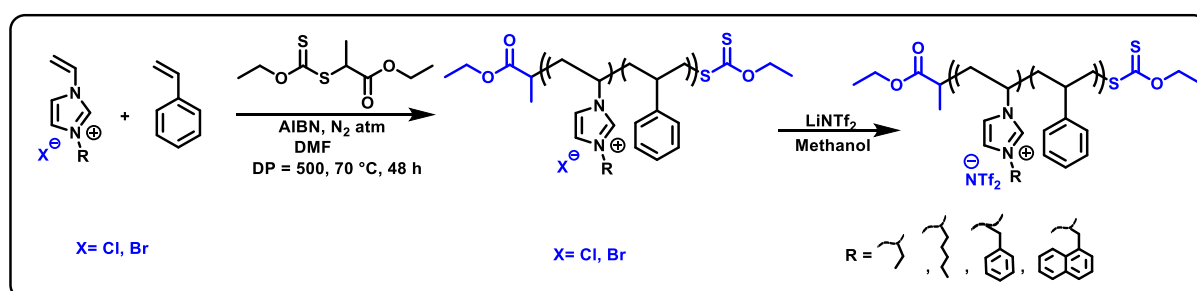
The prepared ionic monomers were polymerized by RAFT polymerization using xanthate-based CTA as shown in Scheme 3. In a typical procedure, 3 g of 1-vinyl-3-benzyl imidazolium bromide (11.29 mmol), 50.21 mg of CTA (0.226 mmol) and 7.42 mg AIBN (0.045 mmol) were taken in a flame dried Schlenk flask and dissolved in 10 mL of dimethylformamide. In order to eliminate any dissolved gases, three freeze thaw cycles were performed. Then, the reaction mixture was heated at 70 °C for 24 h. The obtained white colour poly(ViBenIm)Br was purified by precipitation in cold chloroform and dried under vacuum (2.56 g, 85% yield). The other ionic monomers were polymerized following the same procedure.



**Scheme 3.** RAFT polymerization of vinylimidazolium monomers.

The poly(vinylimidazolium)-polystyrene copolymers were synthesized by RAFT co-polymerization of vinyl monomers with styrene, as shown in Scheme 4. In a typical procedure, 3.2 g (13.05 mmol) of 1-vinyl-3-pentylimidazolium bromide, 1.36 g (13.05 mmol)

of styrene, 11.59 mg of CTA (0.0521 mmol) and 1.7 mg of AIBN (0.059 mmol) were taken in a flame dried Schlenk flask and dissolved in 10 mL of dimethylformamide. In order to eliminate any dissolved gases, three freeze thaw cycles were performed. Then, the reaction mixture was heated at 70 °C for 48 h. The obtained brown colour poly(ViPenIm)(Sty)Br was purified by precipitation in cold chloroform and dried under vacuum (4.52 g, 89% yield). The remaining poly(vinylimidazolium)-polystyrene copolymers were synthesized following the same procedure used for poly(ViPenIm)(Sty)Br [46]. To prepare the poly(ViPenIm)(Sty)NTf<sub>2</sub>, a simple anion metathesis reaction was carried out. Three grams (7.62 mmol) of poly(ViPenIm)(Sty)Br were dissolved in methanol and then an aqueous solution of lithium bis(trifluoromethylsulfonyl)imide (4.37 g, 15.24 mmol) was dropwise added. The mixture was kept for stirring at room temperature for 24 h. The obtained product was washed with an excess amount of water, filtered and dried under vacuum (4.21 g, 93% yield). The anion metathesis reaction of the remaining poly(vinylimidazolium)-polystyrene copolymers were carried out following the same procedure.<sup>46</sup>



**Scheme 4.** Synthesis of the co-poly(ionic liquid)s [ViRIm](Sty)X.

**2.3. Polymer characterization.** Nuclear magnetic resonance (NMR) spectra were recorded on a Bruker AC-400 spectrometer in appropriate deuterated solvents. Differential scanning calorimetry (DSC) experiments were performed using a DSC Q200 instrument from TA. Samples were crimped in non-recyclable aluminium hermetic pans and analysed under nitrogen atmosphere by heating and cooling cycles at a rate of 10 °C min<sup>-1</sup>. Thermal gravimetric analyses (TGA) were carried out using a TGA Q50 instrument from TA. Samples

were heated at a constant rate of  $10\text{ }^{\circ}\text{C min}^{-1}$ , from room temperature to  $600\text{ }^{\circ}\text{C}$ , under a nitrogen atmosphere.

**2.4. Membranes preparation.** The membrane forming ability of the pure PILs and different PIL–IL combinations was evaluated using solvent casting technique, as previously reported [38]. In the case of pure PILs, 12 (w/v)% of PIL solutions were prepared by dissolving an appropriate amount of PIL in acetone. The PIL solutions were stirred at room temperature until complete dissolution of the polymers. The PIL–IL composite solutions in acetone were prepared in a vial by combining appropriate amounts of homo PILs (Scheme 3) or PIL-based copolymers (Scheme 4) with the commercially available  $[\text{C}_2\text{mim}][\text{NTf}_2]$  IL. Then, the solutions were stirred until both PIL and IL were completely dissolved and a homogeneous solution was obtained. All the prepared PIL and PIL–IL solutions were then poured into Petri dishes and left for acetone evaporation during 2 days at room temperature. The solvent evaporation took place slowly and in a saturated solvent environment in order to obtain homogeneous membranes. Finally, to ensure that the solvent was completely evaporated, the membranes were dried at  $45\text{ }^{\circ}\text{C}$  overnight, before gas permeation experiments.

**2.5. Gas permeation experiments.** Ideal gas ( $\text{CO}_2$  and  $\text{N}_2$ ) permeabilities and diffusivities through the prepared membranes were measured, at  $20\text{ }^{\circ}\text{C}$  with a trans-membrane pressure differential of 100 kPa, using the time lag apparatus, which is fully described elsewhere.<sup>47</sup> First, each membrane was degassed under vacuum inside the permeation cell for 12 h. All the permeation data were measured at least in triplicate on a single membrane sample. The permeation cell and lines were evacuated until the pressure was below 0.1 kPa before each run. No residual IL was found inside the permeation cell at the end of the experiments. The membranes thickness (202 to 231  $\mu\text{m}$ ) were measured using a digital micrometer (Mitutoyo,

model MDE-25PJ, Japan). Average thickness was calculated from six measurements taken at different locations of each membrane sample.

Gas transport through the prepared PIL–IL dense membranes was assumed to follow a solution-diffusion mass transfer mechanism,<sup>48</sup> where the permeability ( $P$ ) is related to diffusivity ( $D$ ) and solubility ( $S$ ) as follows:

$$P = D \times S \quad (1)$$

The permeate flux of each gas ( $J_i$ ) was determined experimentally using Eq. (2),<sup>49</sup> where  $V^p$  is the permeate volume,  $\Delta p_d$  the variation of downstream pressure,  $A$  the effective membrane surface area,  $t$  the experimental time,  $R$  the gas constant and  $T$  the temperature.

$$J_i = \frac{V^p \Delta p_d}{AtRT} \quad (2)$$

Ideal gas permeability ( $P_i$ ) was then determined from the steady-state gas flux ( $J_i$ ), the membrane thickness ( $\ell$ ) and the trans-membrane pressure difference ( $\Delta p_i$ ), as shown in Eq. (3).<sup>50</sup>

$$P_i = \frac{J_i}{\Delta p_i / \ell} \quad (3)$$

Gas diffusivity ( $D_i$ ) was determined according Eq. (4). The time lag parameter ( $\theta$ ) was calculated by extrapolating the slope of the linear portion of the  $p_d$  vs.  $t$  curve back to the time axis, where the intercept is equal to  $\theta$ .<sup>50</sup>

$$D_i = \frac{\ell^2}{6\theta} \quad (4)$$

After  $P_i$  and  $D_i$  were known, the gas solubility ( $S_i$ ) was calculated using the relationship shown in Eq. (1). The ideal permeability selectivity (or permselectivity),  $\alpha_{i/j}$ , was obtained by

dividing the permeability of the more permeable specie  $i$  to the permeability of the less permeable specie  $j$ . As shown in Eq. (5), the permselectivity can also be expressed as the product of the diffusivity selectivity and the solubility selectivity:

$$\alpha_{i/j} = \frac{P_i}{P_j} = \left( \frac{D_i}{D_j} \right) \times \left( \frac{S_i}{S_j} \right) \quad (5)$$

### 3. RESULTS AND DISCUSSION

#### 3.1. Synthesis and characterization of imidazolium-based homo and co-PILs.

Imidazolium-based homo and co-PILs were synthesized by RAFT polymerization using CTA as chain transfer agent. The copolymers were synthesized by taking styrene and vinyl imidazolium-based monomers in 1:1 ratio. Even though both monomers were taken in 1:1 ratio, different amount of imidazolium block have seen in copolymer composition probably due to its lower reactivity over styrene. From the  $^1\text{H}$  NMR studies (see Figures S7 to S10 in Supporting Information for further details), the amount of imidazolium block present in the co-PILs was found to be in between 83 and 96% (Table 1). The synthesized polymers bearing Br/Cl as counter-anions were then subjected to anion exchange using LiNTf<sub>2</sub> salt.

The thermal stability of the homo and co-PILs was evaluated by differential scanning calorimetry (DSC) and thermogravimetric analysis (TGA) measurements and the data obtained depicted in Table 1. From the DSC results, it can be observed that the two homo PILs, poly(ViBenIm)NTf<sub>2</sub> and poly(ViNapIm)NTf<sub>2</sub> exhibit  $T_g$  values around -19.8 and 8.6 °C, respectively (Figures. S11 and S12). On the other hand, the four copolymers, poly(ViEIm)(Sty)NTf<sub>2</sub>, poly(ViPenIm)(Sty)NTf<sub>2</sub>, poly(ViBenIm)(Sty)NTf<sub>2</sub> and poly(ViNapIm)(Sty)NTf<sub>2</sub> showed  $T_g$  values of -26.3, 59.4, 97.2 and 95.0°C, respectively (Figures S13 to S16). It can be observed that  $T_g$  is strongly depend on chemical structure of the backbone and side groups. The presence of stiff backbones and bulky side groups in the structure hinders the activation of the backbone segmental motion resulting in a rise in  $T_g$

values.<sup>51</sup> Homo and co-PILs having naphthyl groups in the side chain shown higher  $T_g$  values than those of homo and co-PILs presenting benzyl groups (see Table 1). In the case of co-PIL having pentyl group in the side chain, an higher  $T_g$  value was also found in comparison to that of the co-PIL bearing ethyl group (see Table 1).

Regarding the TGA analysis, the two homo PILs displayed two step decomposition pattern and showed thermal stabilities up to 260 °C, as it can be observed in Figures S17 and S18, respectively. Conversely, the four co-PILs showed one step decomposition pattern with decomposition temperatures between 274 and 304 °C (Figures S19 to S22).

**Table 1** Thermal properties of the prepared homo and co-PILs: decomposition ( $T_{dec}$ ) and glass transition ( $T_g$ ) temperatures.

PILs	% of Imidazolium block <sup>a</sup>	% of styrene block <sup>a</sup>	$T_g$ (°C) <sup>b</sup>	$T_{dec}$ (°C) <sup>c</sup>
Poly(ViBenIm)NTf <sub>2</sub>	100	0	-19.8	266.6
Poly(ViNapIm)NTf <sub>2</sub>	100	0	8.6	259.1
Poly(ViEIm)(Sty)NTf <sub>2</sub>	83	100	-26.3	304.4
Poly(ViBenIm)(Sty)NTf <sub>2</sub>	86	100	97.2	274.0
Poly(ViNapIm)(Sty)NTf <sub>2</sub>	96	100	95.0	283.1
Poly(ViPenIm)(Sty)NTf <sub>2</sub>	95	100	59.4	291.6

<sup>a</sup> Relative percentage of styrene and imidazolium in co-PILs calculated from NMR data.

<sup>b</sup>  $T_{dec}$  defined as the temperature at which the polymer starts fragmentation into smaller molecules.

<sup>c</sup>  $T_g$  defined as the temperature at the middle point of the glass transition region.

**3.2. Membrane forming ability.** Our attempts to prepare free standing membranes with the two synthesized pure homo PILs, namely poly(ViBenIm)NTf<sub>2</sub> and poly(ViNapIm)NTf<sub>2</sub>, were unsuccessful, since they became very brittle and broke even before being peeled out of the Petri dishes. Although the prepared poly(vinylimidazolium)-polystyrene copolymers

showed better film forming ability than the homo PILs, the obtained co-PIL membranes were not flexible enough to be peeled out of the Petri dishes and handled without breaking. Therefore, the incorporation of different amounts of free [C<sub>2</sub>mim][NTf<sub>2</sub>] IL was tested as a strategy to enhance the film forming ability of the homo and poly(vinylimidazolium)-polystyrene copolymers. Also, it is well documented in literature that a large amount of IL incorporated into the PIL leads to higher the CO<sub>2</sub> permeability and diffusivity through the PIL–IL membrane.

**Table 2** Composition of the prepared PIL–IL materials and their ability to be processed into stable and homogenous free standing solid membranes.

PIL	wt% of [C <sub>2</sub> mim][NTf <sub>2</sub> ] (IL)						
	-	10	20	25	30	40	60
Poly(ViBenIm)NTf <sub>2</sub>	✖	γ	γ	-	-	#	-
Poly(ViNapIm) NTf <sub>2</sub>	✖	δ	δ	-	-	δ	#
Poly(ViEIm)(Sty) NTf <sub>2</sub>	✖	#	#	-	-	-	-
Poly(ViPenIm)(Sty) NTf <sub>2</sub>	✖	✓	#	#	#	#	#
Poly(ViBenIm)(Sty) NTf <sub>2</sub>	✖	-	δ	✓	#	#	#
Poly(ViNapIm)(Sty) NTf <sub>2</sub>	✖	-	δ	Δ	✓	#	#

(✖) Brittle, (γ) Sticky, (#) Jelly, (δ) Breaks in to pieces, (✓) Membrane obtained, (-) not performed

Table 2 summarizes the results obtained regarding the ability of PIL-IL combinations to be processed into mechanically stable flat form membranes. As it can be observed, only the PIL–IL materials containing the random copolymers poly(ViPIm)(Sty)NTf<sub>2</sub>, poly(ViBenIm)(Sty)NTf<sub>2</sub> and poly(ViNapIm)(Sty)NTf<sub>2</sub>, combined with 10, 25 and 30 wt% of

IL [C<sub>2</sub>mim][NTf<sub>2</sub>], respectively, resulted in stable and homogenous free standing membranes. The amount of IL needed to obtain stable composite membranes seems to be greatly depend of the co-PIL structure, which can promote different polymer chain arrangements. Table 2 also shows that the synthesized copolymers are in general not able to sustain or accommodate higher amounts of free IL, since the resulting composites turn into gel like-materials. No membrane could be obtained using poly(ViEIm)(Sty)NTf<sub>2</sub> and higher amounts of free IL lead to leaching of the IL from the membrane. Pictures of the co-PIL–IL composite membranes are shown in Figure 2.

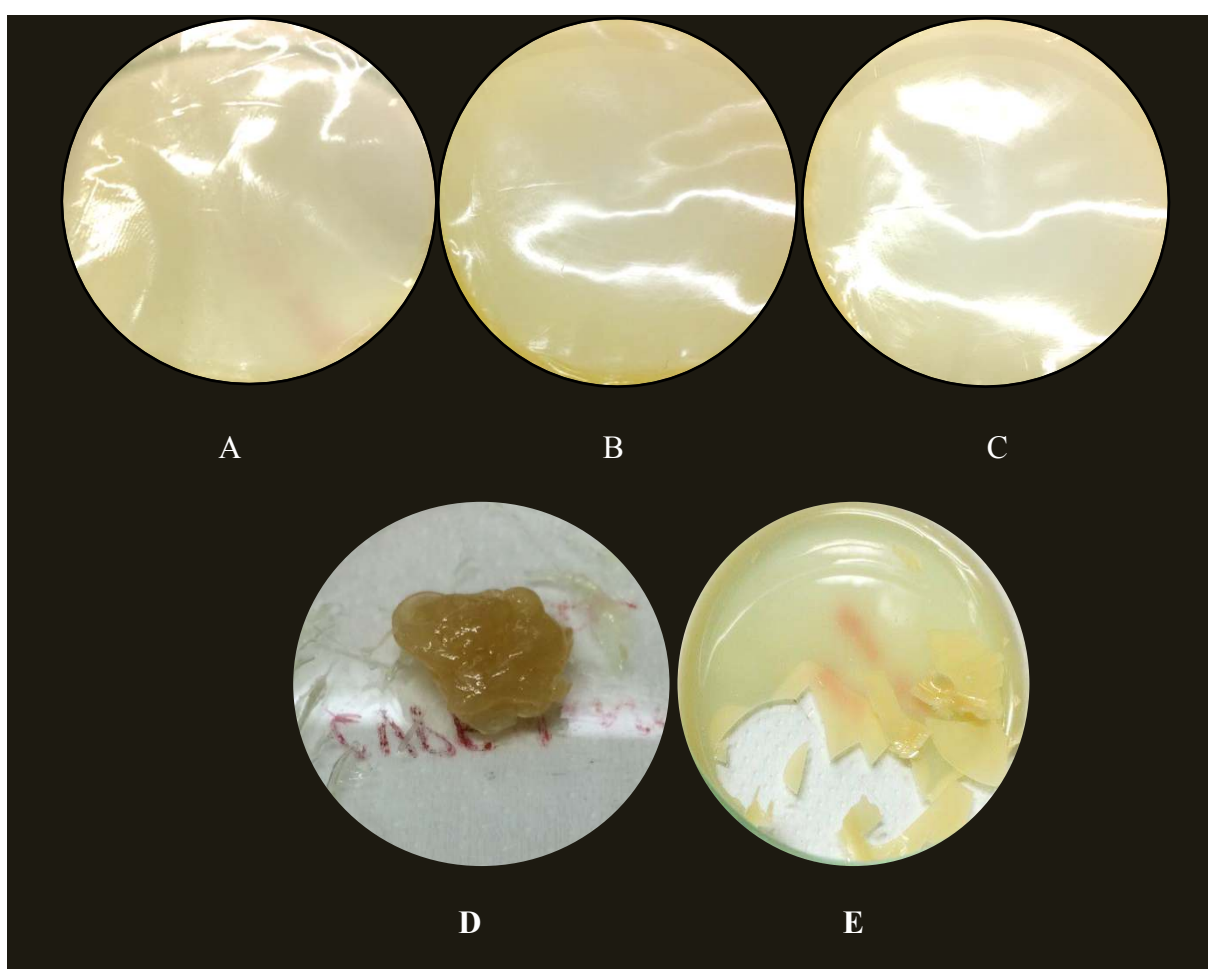


**Figure 2** Pictures of the PIL–IL membranes: (A) poly(ViPenIm)(Sty)NTf<sub>2</sub> with 10 wt% IL, (B) poly(ViBenIm)(Sty)NTf<sub>2</sub> with 25 wt% IL, (C) poly(ViPenIm)(Sty)NTf<sub>2</sub> with 30 wt% IL (D) poly(ViBenIm) NTf<sub>2</sub> with 20 wt% IL (E) poly(ViNapIm) NTf<sub>2</sub> with 20 wt% IL.

**3.3. Gas permeability, diffusivity and solubility.** The gas (CO<sub>2</sub> and N<sub>2</sub>) permeability and diffusivity values, determined using a time lag apparatus, in the co-PIL–IL composite membranes are illustrated in Figures 3 (A) and (B), respectively, while the gas solubility values calculated using Eq. (1) are shown in Figure 3 (C). The CO<sub>2</sub> permeability values were found to be two orders of magnitude higher than those of N<sub>2</sub> in the three co-PIL–IL composite membranes. This observation confirms the membranes' aptitude to separate CO<sub>2</sub> from N<sub>2</sub>. On the other hand, and as expected, the N<sub>2</sub> diffusivities are always higher than those of CO<sub>2</sub>, due to smaller size of the former gas. Regarding gas solubility, a similar behavior to that of gas permeability is observed, since the N<sub>2</sub> solubility values obtained were significantly lower than those of CO<sub>2</sub> amongst the co-PIL–IL composite membranes. Thus, the high CO<sub>2</sub> permeability compared to that of N<sub>2</sub> can be essentially attributed to the high levels of CO<sub>2</sub> solubility relative to N<sub>2</sub>. These findings are in agreement with several studies for CO<sub>2</sub> separation using other PIL–IL composites.<sup>30, 33-35</sup>

The results presented in Figure 3 (A) show that the three co-PIL–IL membranes studied possess similar gas permeabilities. However, and bearing in mind that generally gas permeabilities increase with the free IL content into polymer membranes,<sup>30,37-41</sup> an odd behavior was observed in the present work: the highest gas permeabilities was obtained for the Poly(ViNapIm)(Sty)NTf<sub>2</sub>–30%IL membrane which also has the highest amount of free IL incorporated (30 wt%), while the lowest gas permeabilities were observed for Poly(ViBenIm)(Sty)NTf<sub>2</sub>–25%IL, although Poly(ViPenIm)(Sty)NTf<sub>2</sub>–10%IL is the membrane that contains the lowest amount of free. This behavior suggests that the poly(vinylimidazolium)-polystyrene copolymers structural features have a strong influence on the gas permeation properties of the prepared co-PIL–IL membranes. For instance, the co-PIL having pendant naphthyl group at the imidazolium ring allowed the preparation of a composite membrane with 30 wt% of free IL that has similar CO<sub>2</sub> permeability (~ 24 Barrer)

to that of the composite made with the co-PIL bearing the pentyl as the side chain group (~ 22 Barrer) and only 10 wt% of free IL. In other words, the presence of either the naphthyl or the benzyl group, instead of the pentyl group at the imidazolium ring of the PIL backbone seems to contribute to increase linear chain packing, certainly through  $\pi$ - $\pi$  interactions, contributing for more packed membranes. This large influence of the PIL structural features in the gas permeation properties is probably more marked in these composites that have small amount of IL incorporated that it would be if a large amount of IL could be incorporated.

Another interesting point is that the typical behavior obtained for dense membranes, where the gas permeability is controlled by the gas diffusion is not observed in the present case. Despite the fact that membranes with different poly(vinylimidazolium)-polystyrene copolymers are here compared, it can be seen that gas diffusion follows the order of the IL amount presented in the composite (Figure 3 (B)), thus allowing the conclusion that the liquid like state of the membrane seems to play a more dominant role in gas diffusion. Also to be remarked is the influence of the polycation backbone in the gas solubility results, with the poly(ViPIm)(Sty)NTf<sub>2</sub> exhibiting the highest gas solubility results. In fact, the solubility profile (Figure 3 (C)) obtained for the three studied membranes is similar to the gas permeability (Figure 3 (A)).

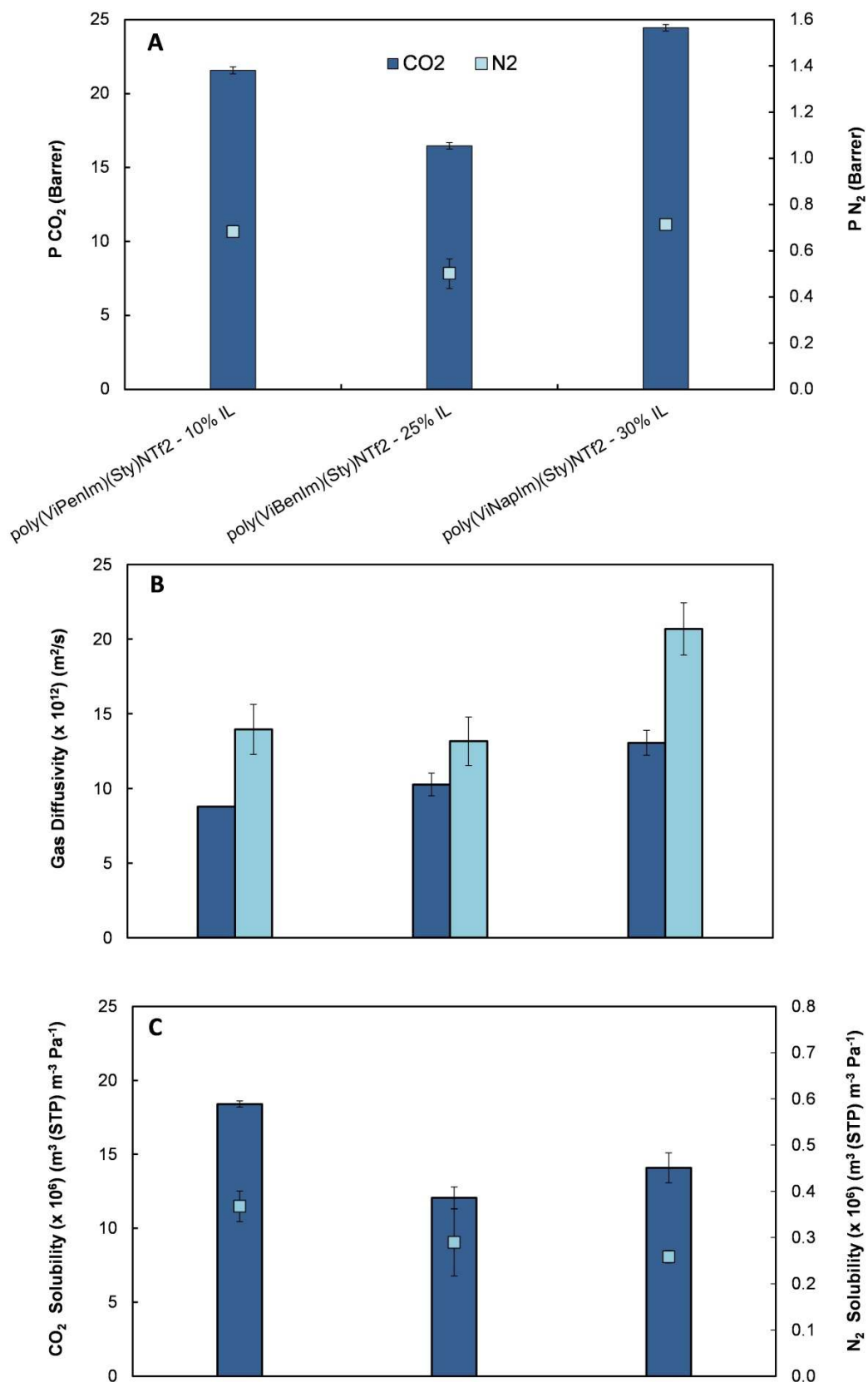


**Figure 3** Gas permeabilities (A), diffusivities (B) and solubilities (C) through the prepared imidazolium-based co-PIL-IL membranes. Error bars represent standard deviations based on three experimental replicas.

**3.4. CO<sub>2</sub>/N<sub>2</sub> separation performance.** The ideal CO<sub>2</sub> permeability and CO<sub>2</sub>/N<sub>2</sub> permselectivity of the co-PIL–IL membranes obtained are listed in Table 3. As it can be seen, the CO<sub>2</sub>/N<sub>2</sub> permselectivities of these membranes are quite similar, with values ranging from 31.7 to 34. Although different poly(vinylimidazolium)-polystyrene copolymers were used, the incorporation of higher amount of free [C<sub>2</sub>mim][NTf<sub>2</sub>] IL slightly increased the CO<sub>2</sub>/N<sub>2</sub> permselectivity of the co-PIL–IL composite membranes by 3.9% and 4.4% in Poly(ViBenIm)(Sty)NTf<sub>2</sub>–25%IL and Poly(ViNapIm)(Sty)NTf<sub>2</sub>–30%IL, respectively, compared to that of the Poly(ViPenIm)(Sty)NTf<sub>2</sub>–10%IL. This is in agreement with the results previously reported for other PIL–IL composite membranes.<sup>33, 36-38, 40, 52</sup>

A comparison of CO<sub>2</sub>/N<sub>2</sub> separation performance between the results obtained in this work and the recently published data for other PIL–IL composite membranes is illustrated in the so-called Robeson plot (Figure 4),<sup>53</sup> which is widely used to evaluate the performance of membrane materials. This plot displays a solid black line, the empirical 2008 upper bound for CO<sub>2</sub>/N<sub>2</sub> gas pair, which is based on a large amount of experimental data for known polymeric membrane materials and illustrates the trade-off between permeability and permselectivity. From Figure 4, it can be observed that the three membranes studied in this work are placed in middle of the Robeson plot. Unfortunately, the results obtained for the co-PIL–IL composite membranes lie below the CO<sub>2</sub>/N<sub>2</sub> upper bound, close to available literature data for other PIL–IL composite membranes made of homo PILs having imidazolium-based backbones and 20 wt% of free IL.

**Table 3** CO<sub>2</sub> permeability ( $P$ ) and CO<sub>2</sub>/N<sub>2</sub> permselectivity ( $\alpha$ ) values of the prepared co-PIL–IL composite membranes. The listed uncertainties represent the standard deviations, based on three experiments.

PIL–IL composite Membranes	Thickness ( $\mu\text{m}$ )	$P$ CO <sub>2</sub> (Barrer)	$\alpha$ CO <sub>2</sub> /N <sub>2</sub>
Poly(ViPenIm)(Sty)NTf <sub>2</sub> – 10% IL	217	21.6 $\pm$ 0.2	31.7
Poly(ViBenIm)(Sty)NTf <sub>2</sub> – 25% IL	231	16.5 $\pm$ 0.2	32.9
Poly(ViNapIm)(Sty)NTf <sub>2</sub> – 30% IL	202	24.5 $\pm$ 0.2	34.4

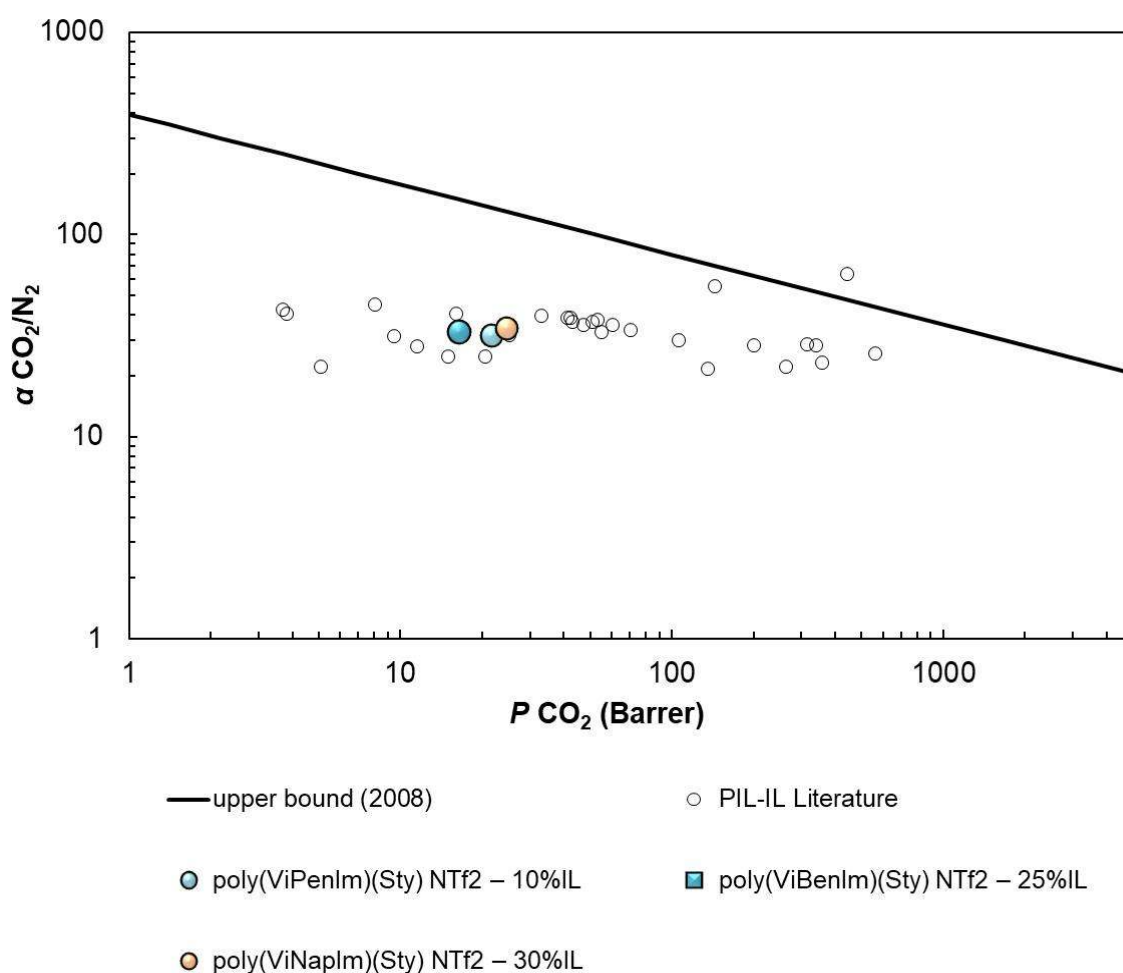


**Figure 4** CO<sub>2</sub>/N<sub>2</sub> separation performance of the co-PIL–IL composite membranes obtained in this work. Data is plotted on a log-log scale and the upper bound is adapted from Robeson.<sup>53</sup> Literature values of other PIL–IL composite membranes previously reported are also illustrated for comparison.<sup>23, 30, 32, 38, 40, 47, 54</sup>

#### 4. CONCLUSIONS

RAFT derived imidazolium-based homo and co-poly(ionic liquid)s were successfully synthesized and anion metathesis reactions were performed. The prepared polymers were characterized by nuclear magnetic resonance (NMR), differential scanning calorimetry (DSC) and thermogravimetric analysis (TGA). The results showed that the synthesized poly(vinylimidazolium)-polystyrene copolymers have high thermal stabilities (up to 300 °C) and are thus suitable for post-combustion CO<sub>2</sub> separation. The membrane forming ability of the prepared imidazolium-based homo and co-poly(ionic liquid)s was evaluated using the solvent casting technique. It was found that the synthesized homo and poly(vinylimidazolium)-polystyrene copolymers were unable to be processed into mechanically stable flat form membranes due to their brittle nature. Consequently, the homo and poly(vinylimidazolium)-polystyrene copolymers were blended with different amounts (10, 20, 25, 30, 40 and 60 wt%) of free [C<sub>2</sub>mim][NTf<sub>2</sub>] IL. Only the random copolymers poly(ViPIIm)(Sty)NTf<sub>2</sub>, poly(ViBenIm)(Sty)NTf<sub>2</sub> and poly(ViNapIm)(Sty)NTf<sub>2</sub>, combined with 10, 25 and 30 wt% of [C<sub>2</sub>mim][NTf<sub>2</sub>], respectively, resulted in stable and homogenous free standing solid membranes. The membranes exhibited CO<sub>2</sub> permeabilities ranging from 16.5 to 24.5 and CO<sub>2</sub>/N<sub>2</sub> permselectivities from 31.7 to 34.4, thus falling in a region of the Robeson plot below the 2008 upper bound, where other PILs bearing similar amount of IL also are. Curiously, and due to the small amount of IL incorporated in the co-PIL–IL composites, the effect of the polymer backbone structure in the gas diffusion and solubility can be observed.

#### ASSOCIATED CONTENT

**Supporting Information.** The NMR, DSC and TGA spectra of the synthesized homo and poly(vinylimidazolium)-polystyrene copolymers are given in Supplementary Information, which is available free of charge online.

## AUTHOR INFORMATION

### **Corresponding Authors:**

Kari Vijayakrishna

Telephone: +91 416 224 2334

Fax: +91 416 224 3092

E-mail: kari@vit.ac.in, vijayakrishnakari@gmail.com

Isabel M. Marrucho

Phone: +351-218413385

E-mail: [isabel.marrucho@tecnico.ulisboa.pt](mailto:isabel.marrucho@tecnico.ulisboa.pt)

### **Notes**

The authors declare no competing financial interest.

## ACKNOWLEDGMENTS

K. Vijayakrishna and N. Pothanagandhi thank “International Research Staff Exchange Scheme (IRSES) 7<sup>th</sup> Framework of European Union People-2012-IRSES” (Project No: 318873), for exchange programme. K. Vijayakrishna also thank DST-SERB, India (Project NO: SR/S1/OC-22/2012) for the financial support. L.C. Tomé is grateful to FCT (*Fundação para a Ciência e a Tecnologia*) for her Post-doctoral research grant (SFRH/BPD/101793/2014). This work was supported by FCT through the project PTDC/CTM-POL/2676/2014 and R&D units UID/Multi/04551/2013 (GreenIT) and UID/QUI/00100/2013 (CQE). This project has received funding from the European Union’s Horizon 2020 research and innovation programme under the Marie Skłodowska-Curie grant agreement No 745734.

## ABBREVIATIONS

$\Delta p_d$	Variation of downstream pressure
$\Delta p_i$	Pressure driving force
$A$	Effective membrane surface area
$\text{CO}_2$	Carbon Dioxide
$D$	Diffusivity
ILs	Ionic Liquids
$J_i$	Steady-state gas flux
$\ell$	Membrane thickness
$\text{N}_2$	Nitrogen
$P$	Permeability
PILs	Poly(ionic liquid)s
$R$	Ideal Gas Law constant
$S$	Solubility
$t$	Time
$T$	Temperature
$V^p$	Permeate Volume
$\alpha_{i/j}$	Permselectivity
$\theta$	Time lag parameter

## REFERENCES

1. Welton, T.; Wasserscheid, P., *Ionic Liquids in Synthesis*. Wiley-VCH Verlag GmbH & Co. KGaA: Weinheim, 2nd edn, 2008.
2. Ueno, K.; Tokuda, H.; Watanabe, M., Ionicity in ionic liquids: correlation with ionic structure and physicochemical properties. *Phys. Chem. Chem. Phys.* **2010**, *12* (8), 1649-1658.
3. Karadas, F.; Atilhan, M.; Aparicio, S., Review on the Use of Ionic Liquids (ILs) as Alternative Fluids for CO<sub>2</sub> Capture and Natural Gas Sweetening. *Energ. Fuel* **2010**, *24* (11), 5817-5828.
4. Ramdin, M.; de Loos, T. W.; Vlugt, T. J. H., State-of-the-Art of CO<sub>2</sub> Capture with Ionic Liquids. *Ind. Eng. Chem. Res.* **2012**, *51* (24), 8149-8177.
5. Huang, Q.; Li, Y.; Jin, X.; Zhao, D.; Chen, G. Z., Chloride ion enhanced thermal stability of carbon dioxide captured by monoethanolamine in hydroxyl imidazolium based ionic liquids. *Energ. Environ. Sci.* **2011**, *4* (6), 2125-2133.
6. Li, X.; Hou, M.; Zhang, Z.; Han, B.; Yang, G.; Wang, X.; Zou, L., Absorption of CO<sub>2</sub> by ionic liquid/polyethylene glycol mixture and the thermodynamic parameters. *Green Chem.* **2008**, *10* (8), 879-884.
7. Qiwei, Y.; Zhiping, W.; Zongbi, B.; Zhiguo, Z.; Yiwen, Y.; Qilong, R.; Huabin, X.; Sheng, D., New Insights into CO<sub>2</sub> Absorption Mechanisms with Amino-Acid Ionic Liquids. *ChemSusChem* **2016**, *9* (8), 806-812.
8. Zeng, S.; Zhang, X.; Bai, L.; Zhang, X.; Wang, H.; Wang, J.; Bao, D.; Li, M.; Liu, X.; Zhang, S., Ionic-Liquid-Based CO<sub>2</sub> Capture Systems: Structure, Interaction and Process. *Chem. Rev.* **2017**, *117* (14), 9625-9673.
9. Seo, S.; DeSilva, M. A.; Xia, H.; Brennecke, J. F., Effect of Cation on Physical Properties and CO<sub>2</sub> Solubility for Phosphonium-Based Ionic Liquids with 2-Cyanopyrrolide Anions. *J. Phys. Chem. B* **2015**, *119* (35), 11807-11814.
10. Gurkan, B. E.; Gohndrone, T. R.; McCready, M. J.; Brennecke, J. F., Reaction kinetics of CO<sub>2</sub> absorption in to phosphonium based anion-functionalized ionic liquids. *Phys. Chem. Chem. Phys.* **2013**, *15* (20), 7796-7811.
11. Zhang, X.; Feng, X.; Li, H.; Peng, J.; Wu, Y.; Hu, X., Cyano-Containing Protic Ionic Liquids for Highly Selective Absorption of SO<sub>2</sub> from CO<sub>2</sub>: Experimental Study and Theoretical Analysis. *Ind. Eng. Chem. Res.* **2016**, *55* (41), 11012-11021.

12. He, W.; Zhang, F.; Wang, Z.; Sun, W.; Zhou, Z.; Ren, Z., Facilitated Separation of CO<sub>2</sub> by Liquid Membranes and Composite Membranes with Task-Specific Ionic Liquids. *Ind. Eng. Chem. Res.* **2016**, *55* (49), 12616-12631.
13. Tomé, L. C.; Patinha, D. J. S.; Ferreira, R.; Garcia, H.; Silva Pereira, C.; Freire, C. S. R.; Rebelo, L. P. N.; Marrucho, I. M., Cholinium-based Supported Ionic Liquid Membranes: A Sustainable Route for Carbon Dioxide Separation. *ChemSusChem* **2014**, *7* (1), 110-113.
14. Tomé, L. C.; Florindo, C.; Freire, C. S. R.; Rebelo, L. P. N.; Marrucho, I. M., Playing with ionic liquid mixtures to design engineered CO<sub>2</sub> separation membranes. *Phys. Chem. Chem. Phys.* **2014**, *16* (32), 17172-82.
15. Chen, S. J.; Zhu, M.; Fu, Y.; Huang, Y. X.; Tao, Z. C.; Li, W. L., Using 13X, LiX, and LiPdAgX zeolites for CO<sub>2</sub> capture from post-combustion flue gas. *Applied Energy* **2017**, *191*, 87-98.
16. Zhonghua, Z.; Xiaoliang, M.; Dongxiang, W.; Chunshan, S.; Yonggang, W., Development of silica-gel-supported polyethylenimine sorbents for CO<sub>2</sub> capture from flue gas. *AIChE J.* **2012**, *58* (8), 2495-2502.
17. Gupta, K. M.; Chen, Y.; Hu, Z.; Jiang, J., Metal-organic framework supported ionic liquid membranes for CO<sub>2</sub> capture: anion effects. *Phys. Chem. Chem. Phys.* **2012**, *14* (16), 5785-5794.
18. Scovazzo, P., Determination of the upper limits, benchmarks, and critical properties for gas separations using stabilized room temperature ionic liquid membranes (SILMs) for the purpose of guiding future research. *J. Membr. Sci.* **2009**, *343* (1-2), 199-211.
19. Uk Hong, S.; Park, D.; Ko, Y.; Baek, I., Polymer-ionic liquid gels for enhanced gas transport. *Chem. Commun.* **2009**, (46), 7227-7229.
20. Jansen, J. C.; Friess, K.; Clarizia, G.; Schauer, J.; Izák, P., High Ionic Liquid Content Polymeric Gel Membranes: Preparation and Performance. *Macromolecules* **2011**, *44* (1), 39-45.
21. Uchytíl, P.; Schauer, J.; Petrychkovych, R.; Setnickova, K.; Suen, S. Y., Ionic liquid membranes for carbon dioxide-methane separation. *J. Membr. Sci.* **2011**, *383* (1-2), 262-271.
22. Bara, J. E.; Hatakeyama, E. S.; Gin, D. L.; Noble, R. D., Improving CO<sub>2</sub> permeability in polymerized room-temperature ionic liquid gas separation membranes through the formation of a solid composite with a room-temperature ionic liquid. *Polym. Adv. Technol.* **2008**, *19* (10), 1415-1420.

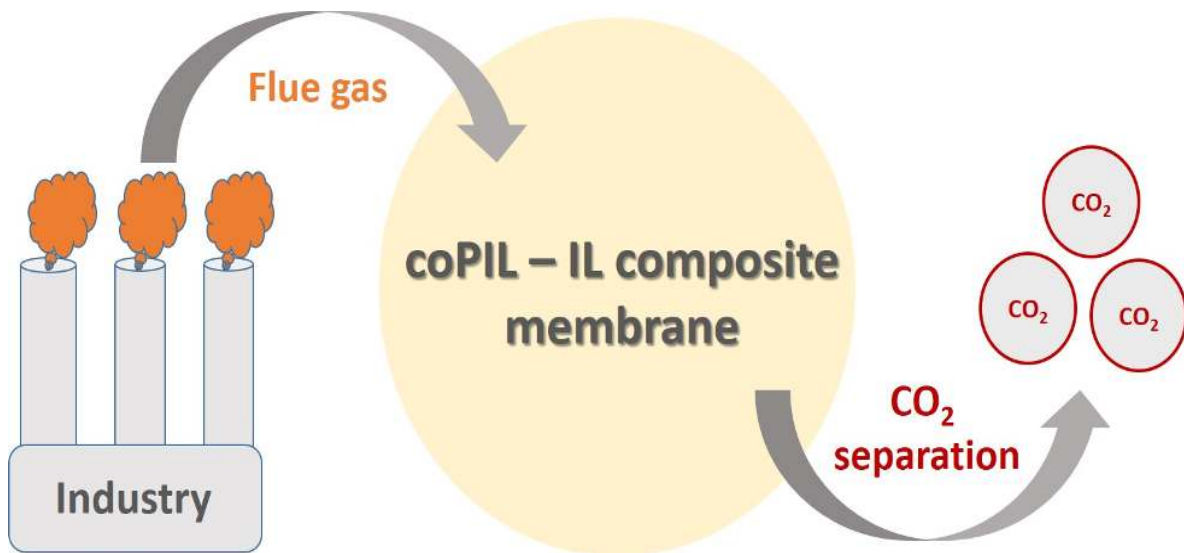
23. Bara, J. E.; Gin, D. L.; Noble, R. D., Effect of Anion on Gas Separation Performance of Polymer–Room-Temperature Ionic Liquid Composite Membranes. *Ind. Eng. Chem. Res.* **2008**, *47* (24), 9919-9924.
24. Tang, J.; Tang, H.; Sun, W.; Radosz, M.; Shen, Y., Poly(ionic liquid)s as new materials for CO<sub>2</sub> absorption. *J. Polym. Sci., Part A: Polym. Chem.* **2005**, *43* (22), 5477-5489.
25. Bara, J. E.; Gabriel, C. J.; Hatakeyama, E. S.; Carlisle, T. K.; Lessmann, S.; Noble, R. D.; Gin, D. L., Improving CO<sub>2</sub> selectivity in polymerized room-temperature ionic liquid gas separation membranes through incorporation of polar substituents. *J. Membr. Sci.* **2008**, *321* (1), 3-7.
26. Camper, D.; Bara, J.; Koval, C.; Noble, R., Bulk-Fluid Solubility and Membrane Feasibility of Rmim-Based Room-Temperature Ionic Liquids. *Ind. Eng. Chem. Res.* **2006**, *45* (18), 6279-6283.
27. Bara, J. E.; Lessmann, S.; Gabriel, C. J.; Hatakeyama, E. S.; Noble, R. D.; Gin, D. L., Synthesis and Performance of Polymerizable Room-Temperature Ionic Liquids as Gas Separation Membranes. *Ind. Eng. Chem. Res.* **2007**, *46* (16), 5397-5404.
28. Tang, J.; Tang, H.; Sun, W.; Radosz, M.; Shen, Y., Low-pressure CO<sub>2</sub> sorption in ammonium-based poly(ionic liquid)s. *Polymer* **2005**, *46* (26), 12460-12467.
29. Tang, J.; Tang, H.; Sun, W.; Plancher, H.; Radosz, M.; Shen, Y., Poly(ionic liquid)s: a new material with enhanced and fast CO<sub>2</sub> absorption. *Chem. Commun.* **2005**, (26), 3325-3327.
30. Tomé, L. C.; Gouveia, A. S. L.; Freire, C. S. R.; Mecerreyes, D.; Marrucho, I. M., Polymeric ionic liquid-based membranes: Influence of polycation variation on gas transport and CO<sub>2</sub> selectivity properties. *J. Membr. Sci.* **2015**, *486* (0), 40-48.
31. Bara, J. E.; Camper, D. E.; Gin, D. L.; Noble, R. D., Room-Temperature Ionic Liquids and Composite Materials: Platform Technologies for CO<sub>2</sub> Capture. *Acc. Chem. Res.* **2010**, *43* (1), 152-159.
32. Bara, J. E.; Noble, R. D.; Gin, D. L., Effect of “Free” Cation Substituent on Gas Separation Performance of Polymer–Room-Temperature Ionic Liquid Composite Membranes. *Ind. Eng. Chem. Res.* **2009**, *48* (9), 4607-4610.
33. Carlisle, T. K.; Wiesenauer, E. F.; Nicodemus, G. D.; Gin, D. L.; Noble, R. D., Ideal CO<sub>2</sub>/Light Gas Separation Performance of Poly(vinylimidazolium) Membranes and Poly(vinylimidazolium)-Ionic Liquid Composite Films. *Ind. Eng. Chem. Res.* **2013**, *52* (3), 1023-1032.

34. Bara, J. E.; Hatakeyama, E. S.; Gabriel, C. J.; Zeng, X.; Lessmann, S.; Gin, D. L.; Noble, R. D., Synthesis and light gas separations in cross-linked gemini room temperature ionic liquid polymer membranes. *J. Membr. Sci.* **2008**, *316* (1-2), 186-191.
35. Kumbharkar, S. C.; Bhavsar, R. S.; Kharul, U. K., Film forming polymeric ionic liquids (PILs) based on polybenzimidazoles for CO<sub>2</sub> separation. *RSC Adv.* **2014**, *4* (9), 4500-4503.
36. Li, P.; Paul, D. R.; Chung, T.-S., High performance membranes based on ionic liquid polymers for CO<sub>2</sub> separation from the flue gas. *Green Chem.* **2012**, *14* (4), 1052-1063.
37. Tomé, L. C.; Aboudzadeh, M. A.; Rebelo, L. P. N.; Freire, C. S. R.; Mecerreyes, D.; Marrucho, I. M., Polymeric ionic liquids with mixtures of counter-anions: a new straightforward strategy for designing pyrrolidinium-based CO<sub>2</sub> separation membranes. *J. Mater. Chem. A* **2013**, *1* (35), 10403-10411.
38. Tomé, L. C.; Isik, M.; Freire, C. S. R.; Mecerreyes, D.; Marrucho, I. M., Novel pyrrolidinium-based polymeric ionic liquids with cyano counter-anions: High performance membrane materials for post-combustion CO<sub>2</sub> separation. *J. Membr. Sci.* **2015**, *483* (0), 155-165.
39. Tomé, L. C.; Marrucho, I. M., Ionic liquid-based materials: a platform to design engineered CO<sub>2</sub> separation membranes. *Chem. Soc. Rev.* **2016**, *45* (10), 2785-2824.
40. Li, P.; Pramoda, K. P.; Chung, T.-S., CO<sub>2</sub> Separation from Flue Gas Using Polyvinyl-(Room Temperature Ionic Liquid)-Room Temperature Ionic Liquid Composite Membranes. *Ind. Eng. Chem. Res.* **2011**, *50* (15), 9344-9353.
41. Carlisle, T. K.; Nicodemus, G. D.; Gin, D. L.; Noble, R. D., CO<sub>2</sub>/light gas separation performance of cross-linked poly(vinylimidazolium) gel membranes as a function of ionic liquid loading and cross-linker content. *J. Membr. Sci.* **2012**, *397-398* (0), 24-37.
42. Hu, X.; Tang, J.; Blasig, A.; Shen, Y.; Radosz, M., CO<sub>2</sub> permeability, diffusivity and solubility in polyethylene glycol-grafted polyionic membranes and their CO<sub>2</sub> selectivity relative to methane and nitrogen. *J. Membr. Sci.* **2006**, *281* (1-2), 130-138.
43. Li, P.; Coleman, M. R., Synthesis of room temperature ionic liquids based random copolyimides for gas separation applications.
44. Chi, W. S.; Hong, S. U.; Jung, B.; Kang, S. W.; Kang, Y. S.; Kim, J. H., Synthesis, structure and gas permeation of polymerized ionic liquid graft copolymer membranes. *J. Membr. Sci.* **2013**, *443* (0), 54-61.
45. Pothanagandhi, N.; Sivaramakrishna, A.; Vijayakrishna, K., Polyelectrolyte-catalyzed Diels-Alder reactions. *React. Funct. Polym.* **2016**, *106*, 132-136.

46. Patinha, D. J. S.; Pothanagandhi, N.; Vijayakrishna, K.; Silvestre, A. J. D.; Marrucho, I. M., Layer-by-layer coated imidazolium – Styrene copolymers fibers for improved headspace-solid phase microextraction analysis of aromatic compounds. *React. Funct. Polym.* **2018**, *125*, 93-100.
47. Tomé, L. C.; Mecerreyes, D.; Freire, C. S. R.; Rebelo, L. P. N.; Marrucho, I. M., Pyrrolidinium-based polymeric ionic liquid materials: New perspectives for CO<sub>2</sub> separation membranes. *J. Membr. Sci.* **2013**, *428* (0), 260-266.
48. Wijmans, J. G.; Baker, R. W., The solution-diffusion model: a review. *J. Membr. Sci.* **1995**, *107* (1-2), 1-21.
49. Matteucci, S.; Yampolskii, Y.; Freeman, B. D.; Pinnau, I., Transport of Gases and Vapors in Glassy and Rubbery Polymers. In *Materials Science of Membranes for Gas and Vapor Separation*, John Wiley & Sons, Ltd: 2006; pp 1-47.
50. Rutherford, S. W.; Do, D. D., Review of time lag permeation technique as a method for characterisation of porous media and membranes. *Adsorption* **1997**, *3* (4), 283-312.
51. Kunal, K.; Robertson, C. G.; Pawlus, S.; Hahn, S. F.; Sokolov, A. P., Role of Chemical Structure in Fragility of Polymers: A Qualitative Picture. *Macromolecules* **2008**, *41* (19), 7232-7238.
52. Tomé, L. C.; Gouveia, A. S. L.; Ab Ranii, M. A.; Lickiss, P. D.; Welton, T.; Marrucho, I. M., Study on gas permeation and CO<sub>2</sub> separation through ionic liquid-based membranes with siloxane-functionalized cations. *Ind. Eng. Chem. Res.* **2017**, *56* (8), 2229-2239.
53. Robeson, L. M., The upper bound revisited. *J. Membr. Sci.* **2008**, *320* (1–2), 390-400.
54. Shaplov, A. S.; Morozova, S. M.; Lozinskaya, E. I.; Vlasov, P. S.; Gouveia, A. S. L.; Tomé, L. C.; Marrucho, I. M.; Vygodskii, Y. S., Turning into poly(ionic liquid)s as a tool for polyimide modification: synthesis, characterization and CO<sub>2</sub> separation properties. *Polym. Chem.* **2016**, *7* (3), 580-591.

# Imidazolium-based co-poly(ionic liquid) membranes for CO<sub>2</sub>/N<sub>2</sub> separation

Nellepalli Pothanagandhi,<sup>a</sup> Liliana C. Tomé,<sup>b,c</sup> Kari Vijayakrishna,<sup>\*a</sup> Isabel M. Marrucho<sup>\*b,c</sup>



“For Table of Contents use only”